Frequency-Based Load Control in Power Systems

Changhong Zhao Ufuk Topcu Steven H. Low

Abstract— **Maintaining demand-supply balance and regulating frequency are key issues in power system control. Conventional approaches focus on adjusting the generation so that it follows the load. However, relying on solely regulating generation is inefficient, especially for power systems where contingencies like a sudden loss in generation or a sudden change in load frequently occur. We present a frequency-based load control scheme for demand-supply balancing and frequency regulation. We formulate a load control optimization problem which aims to balance the change in load with the change in supply while minimizing the overall end-use disutility. By studying the power system model that characterizes the frequency response to real power imbalance between demand and supply, we design decentralized synchronous and asynchronous algorithms which take advantage of local frequency measurements to solve the load control problem. Case studies show that the proposed load control scheme is capable of relatively quickly balancing the power and restoring the frequency under generation-loss like contingencies, even when users only have the knowledge of a simplified system model instead of an accurate one.**

I. Introduction

In power systems, the imbalance between generation and load must get corrected within short periods, otherwise it will drive the power line frequency to deviate from the nominal value (e.g., 60 Hz). Large frequency deviation may threaten the stability and security of the power system, or even worse, cause permanent damage to the facilities [1][2]. Hence balancing generation with load and regulating frequency at the normal level has been a significant topic in power system operations.

Multiple control approaches have been applied to serve these goals. Conventional control efforts focus on the generation side. For example, the automated generation control (AGC) issues signals to control the reserved generation capacity and minimize the area control error (ACE), which includes both frequency deviation and unscheduled tie-line power flows [3][4]. The spinning reserve is a set of frequency responsive generators that automatically increase their output when a sudden loss of supply occurs [3]. In addition, many generators are equipped with speed governors which adjust the mechanical power proportionally to the frequency deviation [5][6]. Other control components include the exciter and the power system stabilizer (PSS) [7].

C. Zhao is with Electrical Engineering, California Institute of Technology, Pasadena, CA 91125, US. E-mail: czhao@caltech.edu.

U. Topcu is with Control and Dynamical Systems, California Institute of Technology, Pasadena, CA 91125, US. E-mail: utopcu@cds.caltech.edu.

S. H. Low is with Computer Science and Electrical Engineering, California Institute of Technology, Pasadena, CA 91125, US. E-mail: slow@caltech.edu.

Generation side control, though widely used, has many inadeqancies. For example, the AGC takes as long as 5-15 minutes to drive the ACE to its setpoint [4]. The spinning reserve generators cannot immediately respond to a contigency, and they must be grid connected and operating in a part-loaded state, thus increasing the cost and emissions [3]. The speed governor typically has a droop characteristic so that it cannot eliminate the steady state frequency deviation [7]. Today, purely relying on the generation control is not only prohibitively expensive but also technically difficult [8]. As a complementary, a lot of works have investigated the potential of load participation in power system control, among which the load control based on local frequency measurement has been highlighted.

Loads are typically controlled via load-shedding, where a whole region of loads are disconnected from the grid by a underfrequency load-shedding (UFLS) relay as a last resort to avoid system failure [2][10]. However, additional granularity can be achieved by individual loads to be controlled. Loads with energy storage, such as heaters, air conditioners, refrigerators and PEVs, can be modulated with reasonable disturbance to customer comforts [9], so they are good candidates for load control. Equipped with frequency sensors, they can sense the frequency as a measure of supply-demand imbalance, and respond in less than 1 second [11].

Schweppe *et al.* presented the idea of individual load control through responding to frequency as early as 1979 [12]. Taylor *et al.* developed a distributed fuzzy load controller for renewable energy systems, which uses both the frequency and the rate of change of frequency to minimize the frequency deviations [13]. Trudnowski *et al.* assumed the loads can be adjusted proportionally to frequency deviations, and investigated multiple issues such as the distribution of loads, time delay and discretized load action [5]. Molina-Garcia *et al.* studied the aggregated load response characteristics when each load is turned on and off as the frequency goes across some thresholds [2]. The Grid Friendly Appliance controller [14] developed by the Pacific Northwest National Laboratory suggests that individual appliances can provide fast reserve within seconds by responding to certain trends in the frequency.

All the works above show the advantage of frequency-based load control that communication between loads and a central controller is no longer essential and the control is decentralized, since each load can measure the frequency signal locally. However, these works are mostly based on experiments, and do not prove convergence of their decentralized schemes. Moreover, they do not consider minimizing end-use disutility caused by changing the loads as a system-

level requirement. An acceptable control strategy should affect end-use functions as little as possible, otherwise users may withdraw from the control program and the reserve capacity may decrease [3].

In this paper, we maintain the advantage that local frequency measurements decentralize the load control. In addition, we formulate a load control optimization problem whose objective is to minimize the overall end-use disutility and whose constraint is the demand-supply power balance. To solve the problem, we develop a synchronous algorithm which assumes all loads sense the frequency without measurement delays and make decisions synchronously, and then consider a more practical asynchronous algorithm which incorporates frequency measurement delay and asynchronous decision making. We prove the convergence of the proposed algorithms by which the load control problem can be solved in a decentralized way. Besides, we discuss the effect of using a simplified system model instead of an accurate one, since in practice users may not get the exact knowledge of the system model and a simplified model can make modeling and computation easier. Numerical experiments show that the proposed load control scheme is able to drive demand-supply imbalance and frequency deviation to zero within 10 to 20 seconds after a sudden generation loss. Moreover, the proposed scheme works well when a simplified system model, instead of an accurate one, is used.

This paper is organized as follows. Section II describes the system model and sets up the load control optimization problem. Section III presents the load control algorithms and proves their convergence. Section IV shows the case studies, including system settings and the results of numerical experiments. Finally, Section V concludes the paper. We skip all the proofs in this paper for the purpose of saving space. Please refer to [15] for the proofs.

II. Model and problem setup

In this section we introduce the power system model upon which the frequency-based load control scheme is built. Then we formulate an optimization problem that describes two goals of load control: minimizing the overall end-use disutility caused by change in load, and balancing demand with supply.

A. System model

Figure 1 shows the schematic diagram of the power system under consideration. On the generator side, multiple control approaches regulate the magnitude of stator voltage $|E_a'|$, the rotor angle δ, the frequency $\omega = d\delta/dt$ and the terminal voltage V_a. For example, the exciter adjusts the field-winding voltage E_{fd} based on the measurement of V_a; the speed governor adjusts the mechanical power P_m based on the measurement of ω. Electrical power P_e is supplied to the load bus via the transmission line. Let $I = \{1,2,...N\}$ denote the set of loads or users (we use these two terms interchangeably). Each load $i \in I$ consumes real power d_i which is regulated by a controller LC_i. Δg denotes a real power disturbance which causes demand-supply imbalance

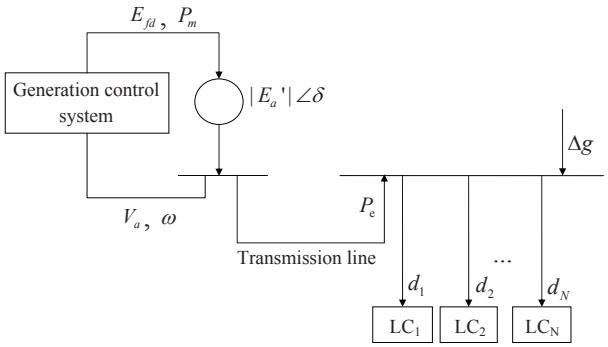

Fig. 1. Schematic diagram of the system under consideration. $|E_a'|$ is the magnitude of generator stator voltage, δ is the rotor angle. The generation control system measures the terminal voltage V_a and frequency ω, and adjusts the field-winding voltage E_{fd} and the turbine mechanical power P_m. P_e is the power supplied to the loads. Each load $i \in \{1,...,N\}$ is equipped with a load controller LC_i that modulates load power d_i when a power disturbance Δg occurs.

and frequency deviation. For example, Δg may be unscheduled power flow from another bus, power supplied by a renewable generation source, a sudden load change, or a sudden generation loss. The case $\Delta g > 0$ may stand for the increase of supply or the decrease of load.

For each $i \in I$, LC_i measures the frequency deviation from the nominal value (e.g., 60 Hz), $\Delta\omega$, and calculates the change in load Δd_i. Let $\Delta d_i > 0$ stand for decreasing the load power, then the total load change is $\Delta d = -\sum_{i\in I}\Delta d_i$. Define $u := \Delta d - \Delta g$, which is actually the demand-supply power imbalance. Then we have a system process that characterizes the relation between frequency deviation $\Delta\omega$ and power imbalance u. We linearize the process around some operating point, get a linear model M and describe M by a transfer function $G(s)$ such that $\Delta\omega(s) = G(s)u(s)$, as is a usual approach to simplify the power system analysis [19][20]. Note that M is continuous-time, while the load control system is a sampling control system, i.e., users sample $\Delta\omega$ and make decisions once every Δt time, and hold their decisions within the sampling interval. We use $t \in T = \{1,2,...\}$ instead of $t = \Delta t, 2\Delta t, ...$ to denote the time. Including the samplers and holders in M, we have a discrete-time realization, denoted by $\{A,B,C\}$, such that

$$\begin{aligned} x_{t+1} &= Ax_t + Bu_t \\ \Delta\omega_t &= Cx_t, \end{aligned} \tag{1}$$

where $x \in \mathbb{R}^n$ is the state vector, $A \in \mathbb{R}^{n\times n}$, $B \in \mathbb{R}^{n\times 1}$, and $C \in \mathbb{R}^{1\times n}$. The load control scheme proposed later requires that $\{A,B,C\}$ is given to the users, and $CB \neq 0$ (see (9)). Hence we make the following assumption, whose reasonability is discussed in [15].

Assumption 1: There exists a discrete-time realization $\{A,B,C\}$ of the system process model M such that $CB \neq 0$.

With the model introduced above, we now formulate an optimization problem that captures the goals of our load control scheme.

B. Load control optimization problem

The goal of the load control scheme proposed here is to balance power demand and supply, i.e., to drive u to zero. By $\Delta\omega(s) = G(s)u(s)$, the frequency deviation will be driven to zero if u is zero. The proposed control scheme simultaneously takes end-use functions as a system-level consideration, by minimizing the overall disutility caused by changing the loads.

We consider a constant Δg, and without loss of generality, assume $\Delta g < 0$. Each user $i \in I$ has a disutility value $D_i(\Delta d_i)$ which is a function of $\Delta d_i \in [0, \overline{d}_i]$, where $\overline{d}_i$ is the maximum change in load i allowed by appliance design or user permission. Considering the goal of minimizing overall disutility and making $u = 0$, given the disturbance Δg and the set of users I, we formulate the following load control problem, denoted by **PP**.

$$\mathbf{PP} \begin{cases} \min\limits_{\Delta d_i \in [0,\overline{d}_i]} & \sum\limits_{i=1}^{N} D_i(\Delta d_i) \\ \text{subject to} & -\sum\limits_{i=1}^{N} \Delta d_i - \Delta g = 0. \end{cases}$$

For feasibility of **PP**, we need $-\sum_{i\in I} \overline{d}_i < \Delta g$, i.e., the magnitude of disturbance does not exceed the capability of changing the loads, which is true if enough loads participate in the load control scheme. We make the following two assumptions on the disutility functions D_i.

Assumption 2: For $i \in I$, D_i is increasing, strictly convex and twice continuously differentiable over $[0, \overline{d}_i]$.

Assumption 3: For $i \in I$, there exists $\overline{\alpha}_i > 0$ so that $D_i''(\Delta d_i) \geq 1/\overline{\alpha}_i$ for $\Delta d_i \in [0, \overline{d}_i]$.

With Assumptions 2-3, **PP** becomes a convex problem which can be solved using the decentralized approach proposed later. Moreover, the reasonability of Assumptions 2-3 can be implied from previous works on demand response, where the utility functions are non-decreasing and concave, which means users are interested to consume more power if possible, and the level of satisfaction for users can gradually get saturated. For example, the utility functions often take the quadratic form and have linear marginal benefits [25][26].

Solving **PP** by a central controller requires the knowledge of D_i for all $i \in I$. However, for privacy considerations, users may not prefer to reveal their disutility functions to the utility company or any other organization that controls the system. Moreover, the disutility functions may take a complex form and change with time, so it would cost much to communicate the disutility fucntions to a central controller. Therefore, we propose a decentralized approach to solve **PP**. In order to derive this decentralized procedure, we consider the dual problem of **PP**. Define the Lagrangian of **PP**

$$L(\Delta d_i, p) := \sum_{i=1}^{N} D_i(\Delta d_i) + p\left(-\sum_{i=1}^{N} \Delta d_i - \Delta g\right).$$

Then, the dual objective function is

$$\begin{aligned} U(p) &= \inf_{\Delta d_i \in [0,\overline{d}_i]} L(\Delta d_i, p) \\ &= \sum_{i=1}^{N} \min_{\Delta d_i \in [0,\overline{d}_i]} (D_i(\Delta d_i) - p\Delta d_i) - p\Delta g. \end{aligned} \tag{2}$$

Hence, we have the dual problem, denoted by **DP**.

$$\mathbf{DP} \begin{cases} \max\limits_{p} \ U(p). \end{cases}$$

The solution to **PP** can be constructed in a decentralized way, from **DP**. To see this, note that given $p \in \mathbb{R}$, the problem

$$\min_{\Delta d_i \in [0,\overline{d}_i]} D_i(\Delta d_i) - p\Delta d_i \tag{3}$$

has a unique minimizer denoted by

$$\Delta d_i(p) = \min\{\max\{(D_i')^{-1}(p), 0\}, \overline{d}_i\}, \tag{4}$$

since D_i is strictly convex. Note that the inverse of D_i' exists over $[D_i'(0), D_i'(\overline{d}_i)]$ since D_i' is continuous and strictly increasing by Assumption 2. Since D_i is convex and **PP** has affine constraints, Slater's condition implies that there is zero duality gap between **PP** and **DP**, and the dual optimal solution, denoted by p^*, is attained [22, Sec. 5.5.3]. It follows that $d(p^*) := [d_1(p^*), ..., d_N(p^*)]^T$ is primal feasible and optimal [22, Sec. 5.5.2]. Therefore, we can focus on solving the dual problem **DP** to solve **PP**, instead of solving **PP** directly.

III. Frequency-based load control algorithms

In this section, we first introduce an input reconstructor which forms the basis of the frequency-based load control algorithms by reconstructing the value of u, which is the input to the system and also the gradient value of the dual objective function, at each load and enabling solving **DP** with a decentralized gradient method. Then we introduce the algorithms, including a synchronous version and an asynchronous version. In the algorithms, each user solves its local problem, so that the changes in the loads converge to the solution of the load control problem **PP**.

A. Input reconstructor

As introduced in Section II-B, given the maximizer of **DP**, denoted by p^*, the optimal change in load i is $\Delta d_i(p^*)$. On the other hand, we can get p^* using the gradient algorithm [17, Sec. 3.2.1], where at each time t the value of p is adjusted in the direction of the gradient $U'(p)$ as

$$p(t+1) = p(t) + \gamma U'(p(t)), \tag{5}$$

where $\gamma > 0$ is a stepsize. Recall that $\Delta d_i(p)$ denotes the unique minimizer of (3) for given p. By (2), if the change in load i at time t is $\Delta d_i(t) = \Delta d_i(p(t))$,[1] we have

$$U'(p(t)) = -\sum_{i=1}^{N} \Delta d_i(t) - \Delta g = u_t, \tag{6}$$

[1]We abuse the notation by referring to $\Delta d_i(\cdot)$ as a function of time on the left of the equation and a function of p on the right. The meaning should be clear from the context.

where u_t denotes the value of demand-supply imbalance u at time t. Substituting (6) into (5) we have

$$p(t+1) = p(t) + \gamma u_t. \tag{7}$$

Therefore, the key to decentralizing the load control is to reconstruct the value of u locally at each load. Since u is the input to the power system modeled by M (see Section II-A), we call the mechanism of reconstructing u as the input reconstructor. In the frequency-based load control scheme, the input reconstructor takes advantage of local frequency measurement, $\Delta\omega$, to reconstruct u. For load $i \in I$, the estimate of the state vector x_t using frequency measurements up to time $(t-1)$ is denoted by $\hat{x}^i_{t|t-1}$, the estimate of x_t using frequency measurements up to time t is denoted by $\hat{x}^i_{t|t}$, and the estimate of u_{t-1} is denoted by $\hat{u}^i_{t-1}$. In the input reconstructor, $\hat{x}^i_{t|t-1}$, $\hat{x}^i_{t|t}$ and $\hat{u}^i_{t-1}$ are recursively given by

$$\hat{x}^i_{t|t-1} = A\hat{x}^i_{t-1|t-1}, \tag{8}$$

$$\hat{u}^i_{t-1} = (CB)^{-1}(\Delta\omega_t - C\hat{x}^i_{t|t-1}), \tag{9}$$

$$\hat{x}^i_{t|t} = \hat{x}^i_{t|t-1} + B\hat{u}^i_{t-1}. \tag{10}$$

The input reconstructor presented by (8)-(10) is a special case of the unbiased minimum-variance input estimator in [21] when process noise and measurement noise are zero. The following proposition states that the input reconstructor is able to reconstruct the value of u locally at each load.

Proposition 1: Suppose Assumption 1 holds, $\hat{x}^i_{0|0} = x_0$. Then, the input reconstructor (8)-(10) gives $\hat{u}^i_{t-1} = u_{t-1}$ for all $i \in I$ at all times $t \in T$.

Based on the input reconstructor, we design decentralized load control algorithms.

B. Synchronous algorithm

In the synchronous algorithm, each user senses the power line frequency without measurement delay, and makes decisions synchronously at times $t \in T = \{1,2,...\}$. The synchronous algorithm forms the basis of the asynchronous algorithm, which will be proposed in Section III-C.

We present the synchronous algorithm as follows.

Algorithm 1: Synchronous frequency-based load control algorithm

For all loads $i \in I = \{1,2,...N\}$, the discrete-time realization of the system process model M, denoted by $\{A,B,C\}$, is given. Choose a stepsize $\gamma > 0$. Set the time $t = 0$, and initialize each load i with $\hat{x}^i_{0|0} = x_0$ and $p_i(0) = 0$.

At times $t = 1,2,...$, load i:

1) Measures the frequency deviation $\Delta\omega_t$, and calculates $\hat{u}^i_{t-1}$ using (8)-(10).
2) Updates the value of p_i as
$$p_i(t) = p_i(t-1) + \gamma\hat{u}^i_{t-1}. \tag{11}$$
3) Determines the change in its load
$$\Delta d_i(t) = \Delta d_i(p_i(t)), \tag{12}$$
where $\Delta d_i(\cdot)$ is given by (4).

For the initialization of the algorithm, we can set $t = 0$ when the system has operated with balanced demand and supply for a relatively long period, and set $\hat{x}^i_{0|0} = 0$ for all i [15]. The stop criterion of the algorithm can be $|\Delta d_i(t+1) - \Delta d_i(t)| < \varepsilon$ for some $\varepsilon > 0$ for all $i \in I$. The algorithm can also run all the time until the system model changes.

To show the convergence of Algorithm 1, we relate it to the gradient algorithm where the dual variable p is adjusted by (7). Starting with $p(0) = 0$, the gradient algorithm produces a sequence $\{p(t), t \in T\}$. Using Algorithm 1, load $i \in I$ generates a sequence $\{p_i(t), t \in T\}$. By (7), (11) and Proposition 1, $p_i(t) = p(t)$ for all $t \in T$, which implies Algorithm 1 is equivalent to the gradient algorithm if the conditions for Proposition 1 hold. Moreover, if Assumptions 2-3 are satisfied, the dual objective function U has the properties which gurantee the convergence of the gradient algorithm. Hence Assumptions 1-3 together lead to the convergence of Algorithm 1. Define $\overline{\alpha} := \max_{i\in I}\overline{\alpha}_i$ (see $\overline{\alpha}_i$ in Assumption 3), and define $\Delta d(t) := [\Delta d_1(t), ..., \Delta d_N(t)]^T$. The following theorem states the convergence of Algorithm 1.

Theorem 1: Suppose Assumptions 1-3 hold and the stepsize γ satisfies

$$0 < \gamma < \frac{2}{\overline{\alpha}N}, \tag{13}$$

then for any $i \in I$, any limit point (at least one exists) of the sequence $\{(\Delta d(t), p_i(t)), t \in T\}$ is primal-dual optimal for problems **PP** and **DP**.

Algorithm 1 assumes an ideal case that all loads sense the frequency without measurement delay and make decisions on the change in their power synchronously at every time $t \in T$. However, this may not be true in practice. Now we come to the asynchronous case, where the frequency measurement may be delayed for a random but bounded time, and not all loads make decisions simultaneously.

C. Asynchronous algorithm

In the asynchronous setting, the frequency deviation $\Delta\omega_t$ at time t is measured by load $i \in I$ at some time within the interval $[t + r(i,t) - 1, t + r(i,t))$, where $r(i,t) \in \mathbb{N}$ is a random number. In the time interval $[t-1,t)$, load i measures a set of frequency deviation signals, denoted by $\Omega_{i,t} = \{\Delta\hat{\omega}^1_{i,t}, ..., \Delta\hat{\omega}^{K_{i,t}}_{i,t}\}$, where $K_{i,t}$ is the number of measured frequency deviation signals ($\Omega_{i,t} = \emptyset$ and $K_{i,t} = 0$ means no frequency deviation signal is measured during $[t-1,t)$). Moreover, load i is able to change its power only at a subset of the times $T = \{1,2,...\}$, denoted by T_i. For the asynchronous algorithm to converge, we make the following two assumptions on $r(i,t)$ and T_i.

Assumption 4: For all $i \in I$, $t \in T$, $l \in \{1,...,K_{i,t}\}$ and $s \in \{1,...,t\}$, if $\Delta\hat{\omega}^l_{i,t}$ is the measurement of $\Delta\omega_s$, then $\Delta\hat{\omega}^{l+1}_{i,t}$ is the measurement of $\Delta\omega_{s+1}$. Moreover, there exists $\overline{r} \in \mathbb{N}$ such that $r(i,t) \le \overline{r}$ for all $i \in I$ and $t \in T$.

Assumption 5: For all $i \in I$, the difference between consecutive elements of T_i is bounded.

Assumption 4 says that the delayed frequency measurements arrive by order. In other words, the frequency deviation signal

that occurs first is measured first by the load. Moreover, all frequency measurement delays are bounded by $\bar{r}$. Assumption 5 says that the time between any consecutive changes of any load is bounded.

With the setting above, we present the asynchronous load control algorithm as follows.

Algorithm 2: Asynchronous frequency-based load control algorithm

For all loads $i \in I = \{1,2,...N\}$, the discrete-time realization of the system process model M, denoted by $\{A,B,C\}$, is given. Choose a stepsize $\gamma > 0$. Set the time $t = 0$, and initialize each load i with $\hat{x}_0^i = x_0$ and $p_i(0) = 0$.

In the time interval $[t-1,t)$ for $t = 1,2,...$, load i:

1) At time $(t-1)$, sets $\hat{x}_{t-1}^i(0|0) = \hat{x}_{t-1}^i$, $p_{t-1}^i(0) = p_i(t-1)$.
2) Once load i measures a new frequency deviation signal $\Delta\hat{\omega}_{i,t}^k \in \Omega_{i,t}$ for $k = 1,...,K_{i,t}$, it calculates $\hat{u}_{t-1}^i(k)$ by

$$\hat{x}_{t-1}^i(k|k-1) = A\hat{x}_{t-1}^i(k-1|k-1)$$

$$\hat{u}_{t-1}^i(k) = (CB)^{-1}(\Delta\hat{\omega}_{i,t}^k - C\hat{x}_{t-1}^i(k|k-1))$$

$$\hat{x}_{t-1}^i(k|k) = \hat{x}_{t-1}^i(k|k-1) + B\hat{u}_{t-1}^i(k),$$

and updates the value of p by

$$p_{t-1}^i(k) = p_{t-1}^i(k-1) + \gamma\hat{u}_{t-1}^i(k).$$

3) At time t, sets $\hat{x}_t^i = \hat{x}_{t-1}^i(K_{i,t}|K_{i,t})$ and $p_i(t) = p_{t-1}^i(K_{i,t})$.
4) If load i is able to change its power at time t, it determines the change

$$\Delta d_i(t) = \Delta d_i(p_i(t)),$$

otherwise, $\Delta d_i(t) = \Delta d_i(t-1)$.

The following theorem states the convergence of Algorithm 2.

Theorem 2: Suppose Assumptions 1-5 hold and the stepsize γ satisfies

$$0 < \gamma < \frac{1}{\overline{\alpha}N/2 + 2\bar{r}},$$

then for any $i \in I$, any limit point (at least one exists) of the sequence $\{(\Delta d(t), p_i(t)), t \in T\}$ is primal-dual optimal for problems **PP** and **DP**.

The proposed load control algorithms are essentially the gradient algorithm, where the gradient of the dual objective function happens to be the system demand-supply imbalance u. Using the input reconstructor, the loads reconstruct the value of u purely from local frequency measurements, without any communication between the loads and a central controller. Hence, no communication delay is involved in the proposed scheme. Moreover, the loads sense the local frequency signals with relatively small measurement delays, and respond within a short period of time. Therefore, the proposed load control scheme is able to relatively quickly balancing the demand and supply and restoring the frequency.

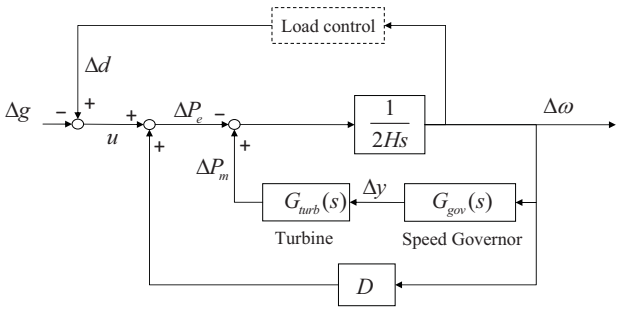

Fig. 2. Core part of the power system model, denoted by M_1. H is the generator inertia constant. D is the damping constant of motor loads. ΔP_e in the change in electrical power. The speed governor adjusts the change in turbine valve opening Δy based on the frequency deviation $\Delta\omega$, then the change in mechanical power ΔP_m is adjusted by the turbine.

IV. Case studies

In this section, we use relatively detailed power system models to evaluate the performance of the proposed load control scheme. Through numerical experiments with generation-loss like contingencies, we compare between the synchronous algorithm and the asynchronous algorithm, and discuss the effect of using a simplified system model instead of an accurate model in the load control scheme.

A. System settings

We now present the power system model under consideration. Figure 2 shows the core part of the model, denoted by M_1, which contains the swing equation, the frequency sensitivity of motor loads and the speed governor. The components in M_1 are major factors that characterize the frequency response caused by demand-supply imbalance [1][6], so we call M_1 as the core part. In M_1, the motion of generator rotor is characterized by the swing equation

$$2H\frac{d\Delta\omega}{dt} = \Delta P_m - \Delta P_e,$$

where H is the inertia constant, ΔP_m is the change in mechanical power and ΔP_e is the change in electrical power. For loads equipped with motors, the power is frequency sensitive, described by

$$\Delta P_e(\Delta\omega) = D\Delta\omega,$$

where D is the damping constant. Moreover, the model contains a speed governor with the transfer function

$$G_{gov}(s) = -\frac{1}{R(1+sT_G)}$$

such that the change in the turbine valve opening $\Delta y(s) = G_{gov}(s)\Delta\omega(s)$. The turbine has a transfer function

$$G_{turb}(s) = \frac{(1+sF_{HP}T_{RH})}{(1+sT_{CH})(1+sT_{RH})}$$

such that $\Delta P_m(s) = G_{turb}(s)\Delta y(s)$. Hence, the transfer function of M_1, denoted by G_1, is

$$G_1(s) = -\frac{1/(2Hs+D)}{1-1/(2Hs+D)G_{turb}(s)G_{gov}(s)}. \quad (14)$$

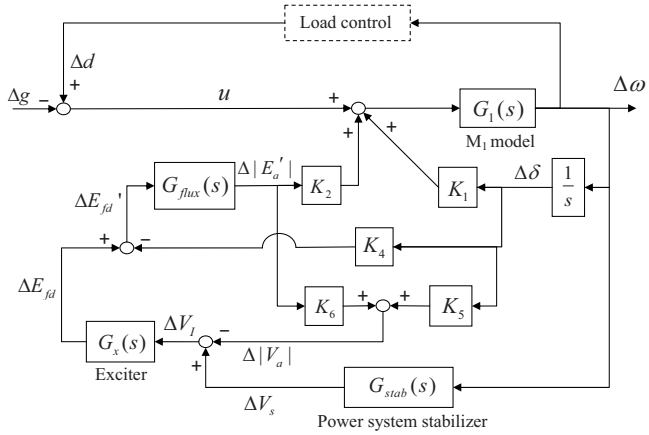

Fig. 3. Complete power system model under consideration, denoted by M_2. M_2 contains M_1. Besides, the exciter adjusts the change in field-winding voltage ΔE_{fd} based on the change in terminal voltage magnitude $\Delta|V_a|$ and a signal ΔV_s from the power system stabilizer. $\Delta\delta$ is the change in rotor angle and $\Delta|E'_a|$ is the change in stator voltage magnitude.

The complete model under consideration, denoted by M_2, is shown in Figure 3. Besides the core part M_1, M_2 contains a power system stabilizer (PSS) with the transfer function

$$G_{stab}(s) = \frac{sK_w(1+sT_1)(1+sT_3)}{(1+sT_w)(1+sT_2)(1+sT_4)},$$

such that a voltage signal $\Delta V_s(s) = G_{stab}(s)\Delta\omega(s)$ is delivered to the exciter. The exciter also receives the change in magnitude of the terminal voltage $\Delta|V_a|$. Here we use an IEEE AC4A exciter, which has the transfer function

$$G_x(s) = \frac{K_A(1+sT_C)}{(1+sT_A)(1+sT_B)}$$

that characterizes the relation between the change in field-winding voltage ΔE_{fd} and the change in exciter input voltage ΔV_I. Moreover, the generator has a flux decay transfer function

$$G_{flux}(s) = \frac{K_3}{1+K_3\tau'_{d0}s}$$

such that the change in stator voltage magnitude $\Delta|E'_a|(s) = G_{flux}(s)\Delta E'_{fd}(s)$, where $\Delta E'_{fd} = \Delta E_{fd} - K_4\Delta\delta$, i.e., the rotor angle $\Delta\delta$ has a negative feedback to the field-winding voltage. We have the transfer function of M_2, denoted by G_2, as

$$G_2(s) = \frac{G_1(s)}{1-G_1(s)[F(s)+K_1/s]},$$

where $G_1(s)$ is given in (14) and $F(s)$ is (omitting the (s) following the transfer functions and variables for simplicity)

$$\begin{aligned} F &= \frac{K_2\Delta|E'_a|}{\Delta\omega} \\ &= \frac{K_2G_{flux}(-K_5G_x/s - K_4/s + G_xG_{stab})}{1+K_6G_{flux}G_x}. \end{aligned}$$

The system under consideration is a per unit system with baseline power $P_{base} = 2000$ MVA. The sampling time is $\Delta t = 0.5$ s. There are N loads in each experiment. Load $i \in I = \{1,2,...,N\}$ has a disutility function $D_i(\Delta d_i) = \Delta d_i^2/(2\overline{\alpha}_i)$, where $\overline{\alpha}_i$ is a random number, e.g., uniformly distributed on $[1,3]$ in our experiments. For $i \in I$, $\Delta d_i \in [0,\overline{d}_i]$, where $\overline{d}_i$ is a positive random number and $\sum_{i\in I}\overline{d}_i = 0.30$ per unit (pu). In the asynchronous setting, the upper bound for all frequency measurement delays is $\overline{r} = 2$ (see Assumption 4 for $\overline{r}$), and the set of decision times of load i is $T_i = T = \{1,2,3,...\}$ for $i \in \{1,...,N/4\}$, $T_i = \{5,10,15,...\}$ for $i \in \{N/4+1,...,N/2\}$, $T_i = \{10,20,30,...\}$ for $i \in \{N/2+1,...,3N/4\}$, and $T_i = \{50,100,150,...\}$ for $i \in \{3N/4+1,...,N\}$. All loads run the load control algorithm with the stepsize $\gamma = 0.9/(\overline{\alpha}N/2+2\overline{r})$, where $\overline{\alpha} = \max_{i\in I}\overline{\alpha}_i$. Therefore, all the sufficient conditions for the convergence of Algorithms 1 and 2 are satisfied. Table I gives the other parameters values used in the case studies.

TABLE I

PARAMETERS USED IN THE CASE STUDIES

Param.	Value	Param.	Value (s)	Param.	Value (s)
K_A	200	H	5	T_1	0.2
K_1	1.0755	T_A	0.04	T_2	0.02
K_2	1.2578	T_B	12	T_3	0.4
K_3	0.3072	T_C	1	T_4	0.04
K_4	1.7124	τ'_{d0}	5.9	T_w	10
Param.	Value	Param.	Value (s)	Param.	Value (pu)
K_5	-0.0409	T_G	0.2	D	1
K_6	0.4971	T_{CH}	0.3	R	0.05
K_w	20	T_{RH}	7	F_{HP}	0.3

B. Experimental results

We use the disturbance Δg which contains two step changes to resemble generation-loss like contingencies, and observe the performance of the proposed load control scheme. Δg is initially zero. At time $t = 2$ s, the first step change occurs with Δg falling by 0.05 pu; at $t = 20$ s, the second step change occurs with Δg falling further by 0.20 pu.

Figure 4 shows the frequency response of the complete system model M_2 to the step changing disturbance, with the synchronous or the asynchronous algorithm. Both algorithms improve the frequency response with small deviations from and quick convergence (within 10 s after the first generation fall and 20 s after the second) to 60 Hz. The synchronous algorithm performs better with even smaller oscillations in transient frequency response than the asynchronous algorithm, because in the synchronous algorithm all the loads are adjusted to the optimal power given the newest gradient value simultaneously at every sampling time, while in the asynchronous algorithm loads get delayed gradient value and some loads are not adjusted at some times.

Now we discuss the effect of using a simplified model instead of an accurate model in the load control scheme. In both Algorithms 1 and 2, a discrete-time realization of the system model, denoted by $\{A,B,C\}$, is given to every load. However, as is mentioned in Section I, users may not get an accurate model, since the utility company may

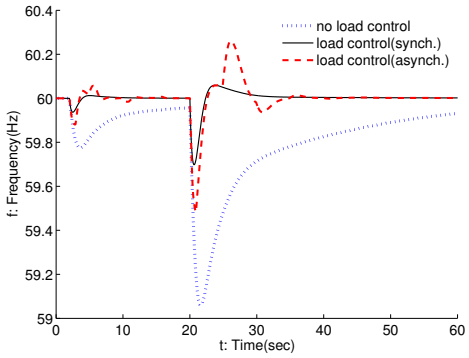

Fig. 4. Frequency reponse with the synchronous or the asynchronous algorithm. The dotted line is the frequency response without load control. The solid line and the dashed line are respectively the frequency response with load control using the synchronous and the asynchronous algorithm.

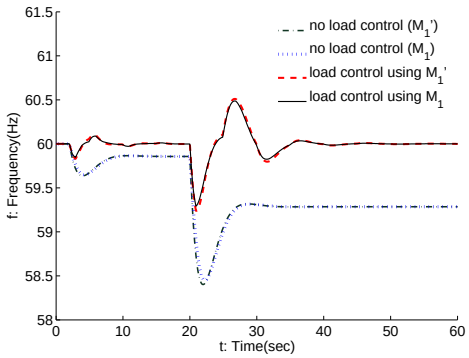

Fig. 5. Frequency reponse of the core part model M_1 and the simplified model M_1'. The dotted line and the dash-dot line are respectively the frequency response of M_1 and M_1' without load control. The solid line and the dashed line are respectively the frequency response of M_1 with load control using M_1 and using M_1'.

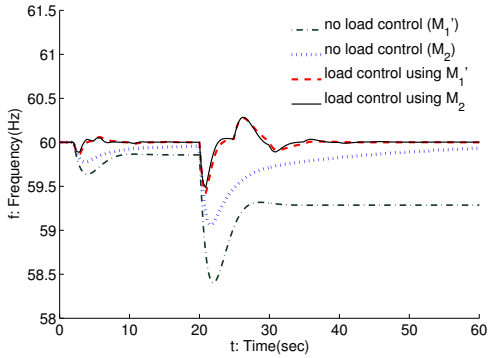

Fig. 6. Frequency reponse with load control schemes using the complete model M_2 and the simplified model M_1'. The dotted line and the dash-dot line are respectively the frequency response of M_2 and M_1' without load control. The solid line and the dashed line are respectively the frequency response with load control schemes using M_2 and using M_1'.

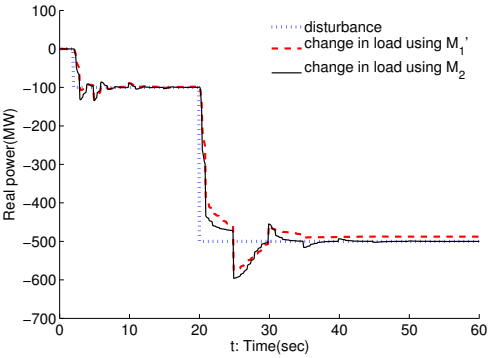

Fig. 7. Total change in load with load control schemes using the complete model M_2 and the simplified model M_1'. The dotted line is the disturbance Δg. The solid line and the dashed line are respectively the total change in load with load control schemes using M_2 and using M_1'.

not reveal the exact system information to the public for security considerations, and the accurate model may be so complicated that it costs much to determine it, deliver it to users and compute with it. Hence, we consider the effect of using a simplified model in the load control algorithm.

For the complete system model M_2, we derive its simplifed model from its core part M_1, since M_1 captures the main characteristics of the frequency response. Note that the transfer function of M_1, denoted by G_1, has a pair of conjugate complex poles which are close to the imaginary axis for the given parameter values. With this condition, we simplify G_1 by discarding poles and zeros that are far from the imaginary axis and canceling zero-pole pairs that are close to each other [24], and have a simplified transfer function

$$\widetilde{G}_1(s) = -\frac{0.1555s + 0.0222}{s^2 + 0.9918s + 0.4666}.$$

which describes a simplified model M_1'. Figure 5 compares the frequency response of M_1 and M_1'. As we can see, M_1' approximates M_1 very well, since its frequency response curve without load control almost overlaps with that of M_1, and the frequency response curves with load control using M_1 and M_1' are quite similar. Hence, M_1' can be regarded as a simplification of the core part model M_1, and a simplification of the complete model M_2.

Figures 6-8 respectively compare the frequency response, the total change in load and the disutility with load control schemes using the complete model M_2 and the simplified model M_1'. Comparing the no-load-control frequency response curves of M_2 (the dotted line) and M_1' (the dash-dot line) in Figure 6, we see that M_1' is not an accurate simplification of M_2. However, the frequency response, the total change in load and the disutility with load control schemes using M_2 and M_1' are still quite close (though there are small steady state differences after the second step change in Figures 7 and 8), which implies the proposed scheme is robust to inaccurate model simplifications. Therefore, it is tolerable to use a simplified system model, instead of an accurate one, in the load control scheme.

V. Conclusion

In this paper, we present a frequency-based load control scheme to balance demand with supply and regulate frequency in power systems. We set up a load control

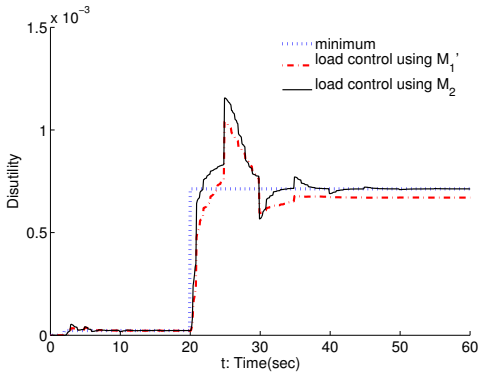

Fig. 8. Disutility caused by load control schemes using the complete model M_2 and the simplified model M_1'. The dotted line is the minimal disutility that can be achieved. The solid line and the dashed line are respectively the disutility caused by load control schemes using M_2 and using M_1'.

optimization problem with the objective of minimizing the total end-use disutility and the constraint of demand-supply power balance. We design decentralized algorithms using local frequency measurements to solve the load control optimization problem, and prove the convergence of the algorithms. Numerical experiments show that the proposed load control scheme is able to relatively quickly balance the power demand with supply and restore frequency under generation-loss like contingencies. In addition, the proposed scheme still has good performance when an inaccurate, simplified system model, instead of an accurate one, is used in the load control algorithm.

ACKNOWLEDGMENT

This work is supported by NSF NetSE grants CNS 0911041, Southern California Edison (SCE), Okawa Foundation, and Boeing Corporation.

REFERENCES

[1] P. M. Anderson and M. Mirheydar, "An adaptive method for setting underfrequency load shedding relays," *IEEE Trans. on Power Systems*, vol. 7, no. 2, pp. 647-655, 1992.

[2] A. Molina-Garcia, F. Bouffard and D. S. Kirschen, "Decentralized demand-side contribution to primary frequency control," *IEEE Trans. on Power Systems*, vol. 26, no. 1, pp. 411-419, 2001.

[3] D. S. Callaway and I. A. Hiskens, "Achieving controllability of electric loads," *Proceedings of the IEEE*, vol. 99, no. 1, pp. 184-199, 2011.

[4] M. Ilic and Q. Liu, "Toward sensing, communications and control architectures for frequency regulation in systems with highly variable resources," *Control and Optimization Theory for Electric Smart Grids*, New York: Springer, 2011.

[5] D. Trudnowski, M. Donnelly and E. Lightner, "Power-system frequency and stability control using decentralized intelligent loads," in *Proc. of the 2005 IEEE T&D Conf. Expo.*, Dallas, TX, May 2006.

[6] J. Dong, J. Zuo, L. Wang, K. S. Kook, I. Chung, Y. Liu, *et al.*, "Analysis of power system disturbance based on wide-area frequency measurements," in *Proc. of the 2007 IEEE Power and Energy Society General Meeting*, Tampa, FL, Jun. 2007.

[7] P. Kundur, *Power System Stability and Control*, New York: McGraw Hill, Inc., 1994.

[8] G. Strbac and ILEX Energy Consulting, *Quantifying the System Costs of Additional Renewables in 2020*. Department of Trade and Industry, London, U.K., 2002.

[9] Z. Xu, J. Ostergaard, M. Togeby, "Demand as frequency controlled reserve," *IEEE Trans. on Power Systems*, vol. 26, no. 3, pp. 1062-1071, 2011.

[10] V. N. Chuvychin, N. S. Gurov, S. S. Venkata and R. E. Brown, "An adaptive approach to load shedding and spinning reserve control during underfrequency conditions," *IEEE Trans. on Power Systems*, vol. 11, no. 4, pp. 1805-1810, 1996.

[11] A. Brooks, E. Liu, D. Reicher, C. Spirakis and B. Weihl, "Demand dispatch: Using real-time control of demand to help balance generation and load," *IEEE Power&Energy Magazine*, vol. 8, no. 3, pp. 21-30, 2010.

[12] F. C. Schweppe, "Frequency Adaptive Power-Energy Re-Scheduler," United States Patent 4317049, 1979.

[13] P. Taylor, "Increased renewable energy penetration on island power systems through distributed fuzzy load control," in *Proc. Int. Conf. Renewable Energies for Islands: Toward 100% RES Supply*, Chania, Greece, Jun. 2001.

[14] PNNL, *Grid Friendly^{TM} Controller Helps Balance Energy Supply and Demand*. [Online]. Available: http://www.gridwise.pnl.gov/docs/pnnlsa36565.pdf.

[15] C. Zhao, U. Topcu and S. H. Low, "Frequency-based load control in power systems," *Technical Report*, California Institute of Technology, 2011. [CaltechCDSTR:2011.007]. Available: http://resolver.caltech.edu/CaltechCDSTR:2011.007.

[16] S. H. Low and D. E. Lapsley, "Optimization flow control, I: Basic algorithm and convergence," *IEEE/ACM Trans. on Networking*, vol. 7, no. 6, pp. 861-874, Dec. 1999.

[17] D. Bertsekas and J. Tsitsiklis, *Parallel and Distributed Computation*. Upper Saddle River, NJ: Prentice Hall, 1989.

[18] D. Bertsekas, *Nonlinear Programming*. Nashua, NH: Athena Scientific, 1995.

[19] A. R. Bergen and V. Vittal, *Power Systems Analysis*, 2nd ed. Upper Saddle River, NJ: Prentice Hall, 2000.

[20] P. M. Anderson and A. A. Fouad, *Power System Control and Stability*, Volume 1. Ames, Iowa: The Iowa State University Press, 1977.

[21] S. Gillijns and B. D. Moor, "Unbiased minimum-variance input and state estimation for linear discrete-time systems," *Automatica*, vol. 43, no. 1, pp. 111-116, 2007.

[22] S. Boyd and L. Vandenberghe, *Convex Optimization*, U.K.: Cambridge University Press, 2004.

[23] L. Gan, U. Topcu and S. H. Low, "Optimal decentralized protocols for electric vehicle charging," to appear in *Proc. 2011 IEEE Conf. Decision and Control*, Orlando, FL, Dec. 2011.

[24] K. J. Astrom and R. M. Murray, *Feedback Systems: An Introduction for Scientists and Engineers*, Princeton, NJ: Princeton University Press, 2008.

[25] N. Li, L. Chen and S. H. Low, "Optimal demand response based on utility maximization in power networks," in *Proc. of the 2011 IEEE Power and Energy Society General Meeting*, Detroit, MI, Jul. 2011.

[26] P. Samadi, A. Mohsenian-Rad, R. Schober, V. W. S. Wong, and J. Jatskevich, "Optimal real-time pricing algorithm based on utility maximization for smart grid," in *Proc. 2010 IEEE SmartGridComm*, Gaithersburg, MD, Oct. 2010.